

Age-Specific Experimental and Computational Calibration of Thyroid in vivo Monitoring

T. Beaumont, Dago Pacôme Onoma, Maeva Rimlinger, David Broggio, Pedro Caldeira Ideias, Didier Franck

▶ **To cite this version:**

T. Beaumont, Dago Pacôme Onoma, Maeva Rimlinger, David Broggio, Pedro Caldeira Ideias, et al.. Age-Specific Experimental and Computational Calibration of Thyroid in vivo Monitoring. IEEE Transactions on Radiation and Plasma Medical Sciences, 2019, 3 (1), pp.43-46. 10.1109/TRPMS.2018.2829931 . irsn-04021252

HAL Id: irsn-04021252
https://irsn.hal.science/irsn-04021252

Submitted on 9 Mar 2023

HAL is a multi-disciplinary open access archive for the deposit and dissemination of scientific research documents, whether they are published or not. The documents may come from teaching and research institutions in France or abroad, or from public or private research centers.

L'archive ouverte pluridisciplinaire **HAL**, est destinée au dépôt et à la diffusion de documents scientifiques de niveau recherche, publiés ou non, émanant des établissements d'enseignement et de recherche français ou étrangers, des laboratoires publics ou privés.

Age-specific experimental and computational calibration of thyroid *in vivo* monitoring

T. Beaumont[1,*],P. Onoma[1], M. Rimlinger[1], D. Broggio[1], P. Caldeira Ideias[2] and D.Franck[3]
[1,*]Institut de Radioprotection et de Sûreté Nucléaire (IRSN), PSE-SANTE/SDOS/LEDI, Fontenay-aux-Roses, France
[2,*]Institut de Radioprotection et de Sûreté Nucléaire (IRSN), PSE-ENV/SIRSE/LSE, Le Vésinet, France
[3,*]Institut de Radioprotection et de Sûreté Nucléaire (IRSN), PSE-SANTE/SDOS, Fontenay-aux-Roses, France

*Corresponding author: tiffany.beaumont@irsn.fr

***Abstract* — Age-specific thyroid phantoms corresponding to 5, 10, 15 years-old and the adult case have been designed and manufactured with a 3D printer. Reference measurements of the counting efficiency have been carried out for thyroid in vivo monitoring of ^{131}I with all these phantoms. These measurements where performed for the emergency mobile units of IRSN. The full efficiency curve, between 29 and 1000 keV, was then obtained by Monte-Carlo calculations and validated by comparison of a large set of measurements. The obtained efficiency curves are consistent and show that the relative difference in efficiency between the adult and the children case are energy dependent.**

***Index Terms*— Monte-Carlo, in vivo measurement, thyroid, phantom, children**

I. INTRODUCTION

IN case of accidental nuclear release ^{131}I is of major concern for thyroid cancer induction, particularly for children.

Currently, detectors for in vivo monitoring are calibrated with an adult thyroid phantom which induces non negligible measurement uncertainties for children. In order to improve the radio-iodine uptake measurement for children a set of realistic thyroid phantoms corresponding to different ages has been developed using CAD software and 3D printed.

In a previous work [1] this set has been used to measure age specific counting efficiency of the NaI(Tl) detectors of the light emergency mobile units of IRSN [2]. For that purpose ^{133}Ba was used as a surrogate of ^{131}I and a single efficiency value was obtained at the photopeak energy of ^{133}Ba. However, in the emergency vehicles, for the measurements processing to be fully automated, it is needed to have an energy efficiency curve and not a single efficiency value.

In order to obtain this curve Monte Carlo calculations have been carried out to compute the full efficiency curve, spanning energy between 29 keV and 1 000 keV. When this study was carried out it was not possible to fill-in the thyroid phantoms with multi-gamma liquid sources because we would have then exceeded the legal threshold for radionuclide possession.

II. MATERIALS AND METHODS

A. *Age-specific thyroid phantoms*

Thyroid phantom adapted to 5, 10, 15 years-old children and to adults have been designed and manufactured in a previous study [1] (see Figure 1).

A simple but realistic thyroid shape proposed by Ulanovsky was selected since it is age-dependent and was previously used by the MIRD committee. For modeling, we used the equations and parameters given in [3]-[5]. Using these parameters age-dependent thyroid volumes differed by about 3% of those recommended by [6] and we thus applied 3D scaling factors to match the requested volumes. Necks, vertebrae, spinal cords and tracheas were also designed according to age, to create the final phantom. The exact dimensions of the phantoms were fixed taking into account the absorption properties of the material, i.e. by calculation of equivalent thicknesses [1].



Figure 1. Age-specific thyroid phantoms corresponding to (left to right) an adult, 15 years-old teenager and 10 and 5 years-old children.

Based on these dimensions, the age-specific thyroid phantoms were modeled. After 3D printing the thyroid inserts as shown in Figure 1 are obtained, they are filled with a radioactive solution of ^{133}Ba.

B. *Sodium Iodine Detector*

The sodium iodine (NaI(Tl)) detector considered in this study is used in IRSN mobile units for thyroid measurements in case of emergency, typically a reactor accident affecting a large population. The fleet of mobile units is described elsewhere [2].

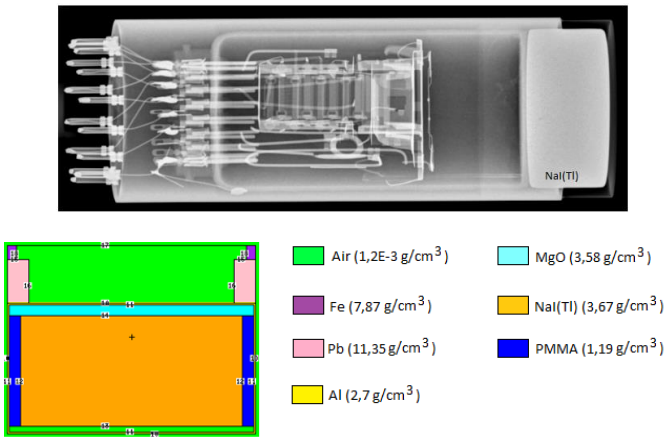


Figure 2. Radiography of the NaI(Tl) detector and its Monte-Carlo model.

The detector model is a 51B25/2M from Scionix, it consists of a 2"x1" crystal encapsulated in 0.4 mm aluminum crystal housing. An additional 1 cm thick lead collimator is placed on the front of the entrance window. The entrance window is made of aluminum with a diameter of 47 mm and is separated from the crystal by 2.4 mm of drying material.

Figure 2 shows the radiography of the NaI(Tl) detector and the MCNP model of this detector.

C. Measurement of counting efficiency

The counting efficiency was measured with the age specific phantoms filled with a ^{133}Ba solution used in a previous work [1]. These measurements are then used to assess the quality of the Monte-Carlo simulation. For a gamma-line of energy *E* the counting efficiency is defined as follows [7]:

$$\varepsilon(E) = N(E) / (t y_i A) \qquad (1)$$

where *A* is the source activity (Bq), *N(E)* is the net number of counts in the photoelectric peak at energy E, y_i the yield of the gamma-ray and *t* the counting time.

To obtain the net number of counts in the photoelectric peak the scattered component is subtracted. For that purpose the left and right part of the photopeak are used to fit a linear continuum describing the scattered component [7].

Here we measured the counting efficiency at 81 keV and 356 keV and for several distances between the detector and the phantom ranging from 0 cm (contact) to 15 cm.

All measurements were taken with the detector centered at the isthmus location; special positioning sheets were prepared on tracing and graph paper to ensure equivalent positioning of all the measurements and reproducibility of measurements (see Figure **3**). The measurements were carried out for all the thyroid phantoms (5, 10, and 15 years-old and adult).

D. Numerical calibration

1) Monte-Carlo simulation of the counting efficiency

MCNP was used to determine the counting efficiencies of the NaI(Tl) detector. Gamma ray energies emitted by ^{241}Am (59.5 keV), ^{133}Ba (81 keV and 356 keV), ^{57}Co (122 keV) and

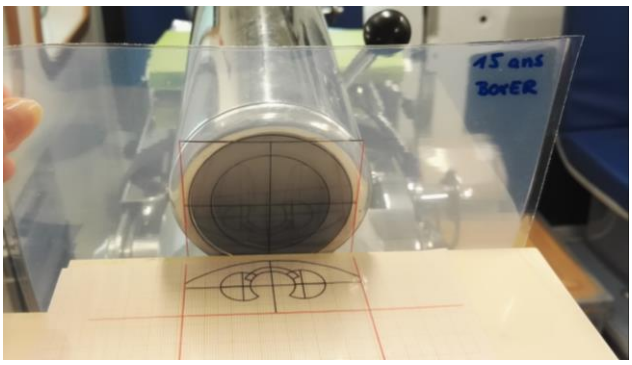


Figure 3. Picture showing the tracing and graph papers enabling reproducible possitionning of thyroid phantoms in front of the detector.

^{137}Cs (662 keV) were used to calculate the counting efficiencies and to deduce the efficiency calibration curves of the NaI(Tl) detector. Additional energies of 29 keV and 1000 keV were also considered. Each counting efficiency was calculated in a separate MCNP run where only the energy of interest was considered.

The F8 tally was used to simulate the pulse height spectrum in the NaI(Tl) crystal. The number of photon generated in each calculation was at least 10^6 giving a statistical uncertainty of less than 1 %. The MCNP default options were used for the "mode p"; no special energy cut nor special physic model were used.

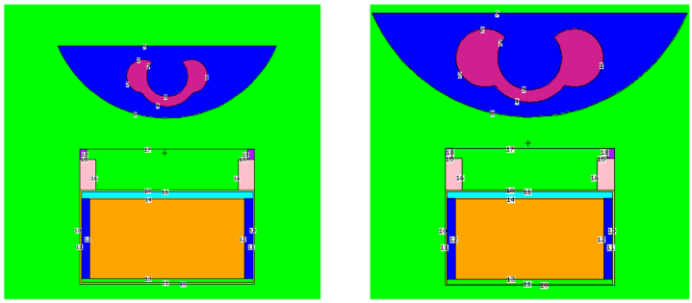


Figure 4. Illustration of *in vivo* thyroid simulation at 1 cm (left) for the 5 years old and (right) for the adult.

From the calculated counting efficiencies, an efficiency calibration curve was fitted, for each phantom, using the following exponential curve fitting function:

$$\varepsilon = \exp[\, a.\ln^4(E) + b.\ln^3(E) + c.\ln^2(E) + d.\ln(E) + e] \qquad (2)$$

where ε is the counting efficiency, E is the energy in keV and where the fitting parameters are a, b, c, d and e. This kind of fitting function, even if it lacks of theoretical basis, is known to describe well the efficiency curve of scintillation and semi-conductor detectors [8],[9].

The fitting procedure was applied for each phantom.

2) Validation

To validate the Monte-Carlo simulations the computed and experimental efficiencies at 81 and 356 keV were compared. For this specific task of validation 11 counting distance for

measurement and simulation were used, between contact (0 cm) and 15 cm.

III. Results

A. Validation

Table 1 and 2 show the relative deviation, in percent, between the measured and calculated efficiencies at 81 and 356 keV. A positive value indicates that the simulation overestimates the measurement. The maximum deviation at 356 keV was found for the 5-years old case at a counting distance of 15 cm (9.8%). The maximum deviation at 81 keV was found for the 5-years old case at a counting distance of 15 cm (-16%). On average (over all distances) the difference in counting efficiency is around -3% at 81 keV and around 5% at 356 keV.

TABLE 1.
RELATIVE DIFFERENCES (%) BETWEEN MEASURED AND CALCULATED COUNTING EFFICIENCY FOR 4 THYROID PHANTOMS AND ALL PHANTOMS-DETECTOR DISTANCES

Distance	5 years	10 years	15 years	Adult
0	7.9	5.4	5.1	4.3
1	2.2	4.3	1.9	1.7
1.5	0.5	-0.2	0.7	-0.1
2	7.1	-1.3	-1.6	-1.5
3	-0.3	-1.3	-2.8	-1.7
4	-1.6	-1.9	-0.8	-2.0
6	-5.8	-0.9	-6.1	-4.1
8	-6.6	-7.7	-6.1	-10.0
10	-10.8	-7.8	-8.6	-7.3
12.5	-15.3	-9.9	-7.5	-12.3
15	-15.7	-8.1	7.3	1.4

TABLE 2.
RELATIVE DIFFERENCES (%) BETWEEN MEASURED AND CALCULATED COUNTING EFFICIENCY AT 356 KEV FOR 4 THYROID PHANTOMS AND ALL PHANTOM-DETECTOR DISTANCES

Distance	5 years	10 years	15 years	Adult
0	8.5	4.8	3.3	4.0
1	6.4	7.2	3.4	3.5
1.5	8.2	7.9	5.0	4.0
2	6.4	6.3	3.7	1.5
3	3.2	8.4	2.0	0.9
4	5.6	4.5	1.6	3.0
6	4.3	4.1	2.3	5.8
8	7.8	7.4	4.0	4.1
10	3.6	9.2	3.2	-1.0
12.5	6.3	7.5	4.4	2.5
15	9.8	8.1	3.2	9.0

B. Age specific counting efficiency curves

The calculated efficiencies and the fitting curves are shown in Figure 5 for the full energy range and all the phantoms. Table 3 gives the parameters used for the fitting procedure.

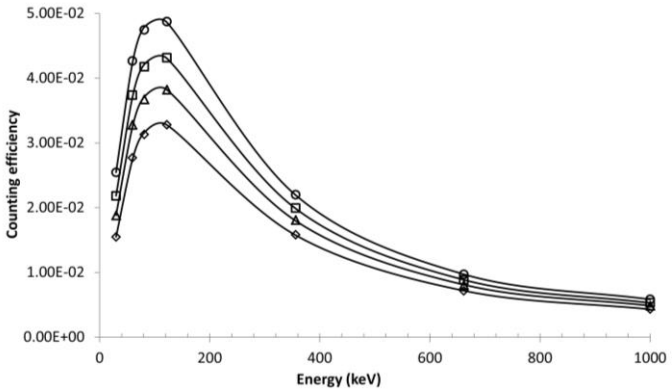


Figure 5. Fitted calibration curves (top to bottom) for 5 years-old, 10 years-old, 15 years-old and adult and calculated efficiencies (symbols).

TABLE 3.
PARAMETERS USED FOR THE FITTING OF EFFICIENCY CURVES

	5 years	10 years	15 years	Adult
a	0.04	0.04	0.04	0.04
b	-0.84	-0.79	-0.78	-0.74
c	5.55	5.18	5.10	4.82
d	-14.64	-13.42	-13.13	-12.13
e	9.10	7.43	6.88	5.37

IV. Discussion

A. Validation of Monte-Carlo modelling

The validation of the modelling at two energies is rather robust since it takes into account 11 counting distances. The difference between calculation and experiment, for distance less than 8 cm, is less than 10%. In similar work of efficiency calculations better results are sometimes obtained [10], [11]. Here most of the relatively large differences occur at large counting distances. It also appears that for the 5 years old phantom the agreement is in general worse than for the other phantoms. It can be suspected that for the 5 years old phantom there is a small error in the activity put in the phantom. At large distance, for all phantoms, the difference might be due to a misalignment of the phantom and detector, hence a difference of positioning between experiment and simulations. However, for the purpose of emergency measurements we can consider that such an uncertainty is acceptable.

B. Calibration curves

As expected the calibration curves present a maximum around 120 keV, a sharp decrease at low energy and a slow decrease at high energy. More importantly, the calibration curves for different ages do not cross. We also note that the bigger the volume the lower the efficiency, which is explained by the concentration of the radioactive source in a smaller volume [12].

The efficiency curves also show that the relative efficiency difference, between phantoms representing different ages, is energy dependent. For example, at 356 keV the efficiency difference between the 5 years-old case and the adult is 40%, while it is 51% at 81 keV. If age-specific calibration factors are not used, application of a default adult calibration will directly lead to an overestimate of the dose.

Here the calibration curves have been calculated for a counting distance of 1 cm. This choice might not exactly reflect the counting position at contact, used for adults, but for young children it is a reasonable assumption since the size of detectors might prevent a measurement at contact. For other counting distance a similar trend of efficiency curves is expected, even if for very long counting distance it is expected that the effect of thyroid volume will be less pronounced.

V. Conclusion

The developed thyroid phantoms enabled to obtain age specific calibration factors for emergency in vivo monitoring of children. Since the thyroid of children is more radiosensitive than adults it is of great interest to reduce the sources of uncertainties affecting the dose assessment of this population.

Taking into account the size of thyroid for uptake measurement might be also useful in nuclear medicine department. Indeed, the treatment of benign thyroid disease, like Grave's disease, requires a personalized dosimetry and hence personalized thyroid retention function. When this latter is established by spectroscopic measurement, the retention at a given time is calculated from an efficiency obtained with a ANSI like phantom. Taking into account the size of the thyroid might improve the assessment of the retention function since significant variations between thyroid volumes are found for patients treated in nuclear medicine department.

Acknowledgment

The Bicêtre Hospital (APHP) specifically Jad Farah for his help for the radiography of the NaI(Tl) detector.

The LAMIV team, specifically Jean-Pierre Heuze, Didier Viltard, Etienne Anthony and Isabelle Vu for their help for *in vivo* measurements.

References

[1] T. Beaumont, P. C. Ideias, M. Rimlinger, D. Broggio, and D. Franck, "Development and test of sets of 3D printed age-specific thyroid phantoms for 131 I measurements," Phys. Med. Biol., vol. 62, no. 12, pp. 4673–4693, 2017.

[2] D. Franck et al., "Development of a fleet of intervention mobile unit for radiological accident monitoring of internal contamination (2012) Proceedings of IRPA13 May 2012, Glasgow (full paper TS2b.5)," 2012.

[3] A. V. Ulanovsky and K. F. Eckerman, "Absorbed fractions for electron and photon emissions in the developing thyroid: fetus to five years old," Radiat. Prot. Dosimetry, vol. 79, no. 1–4, pp. 419–423, 1998.

[4] A. V. Ulanovsky, V. F. Minenko, and S. V. Korneev, "Influence of Measurement Geometry on the Estimate of 131I Activity in the Thyroid: Monte Carlo Simulation of a Detector and a Phantom.," Health Phys., vol. 72, no. 1, pp. 34–41, 1997.

[5] A. Gardumi, J. Farah, and A. Desbree, "Creation of ORNL NURBS-based phantoms: evaluation of the voxel effect on absorbed doses from radiopharmaceuticals," Radiat. Prot. Dosimetry, vol. 153, no. 3, pp. 273–281, Mar. 2013.

[6] ICRP, "Basic Anatomical and Physiological Data for Use in Radiological Protection Reference Values. ICRP Publication 89," Ann. ICRP, vol. 32, no. 3–4, 2002.

[7] ICRU, "Direct Determination of the Body Content of Radionuclides" *ICRU Report 69,* 2003.

[8] Gordon R. Gilmore, Practical Gamma-ray Spectrometry. John Wiley & Sons, 2008.

[9] R Casanovas, J. J. Morant and M. Salvadó, "Development and calibration of a real-time airborne radioactivity monitor using direct gamma-ray spectrometry with two scintillation detectors" Applied Radiation and Isotopes, vol. 89, pp. 102-108, 2014.

[10] T. Vrba et al., "EURADOS intercomparison exercise on MC modeling for the in-vivo monitoring of Am-241 in skull phantoms (Part I)," Radiat. Phys. Chem., vol. 104, pp. 332–338, Nov. 2014.

[11] D. Broggio et al., "Monte Carlo modelling for the in vivo lung monitoring of enriched uranium: Results of an international comparison," Radiat. Meas., vol. 47, no. 7, pp. 492–500, Jul. 2012.

[12] J. Farah, D. Broggio, and D. Franck, "Female workers and in vivo lung monitoring: A simple model for morphological dependence of counting efficiency curves," Phys. Med. Biol., vol. 55, no. 23, pp. 7377–7395, 2010.